

## Polymer Layered Silicate/Carbon Nanotube Nanocomposites: Morphological and Rheological Properties

*S. Peeterbroeck,<sup>1</sup> M. Alexandre,<sup>1</sup> J. B. Nagy,<sup>2</sup> N. Moreau,<sup>2</sup> A. Destrée,<sup>2</sup> F. Monteverde,<sup>3</sup> A. Rulmont,<sup>4</sup> R. Jérôme,<sup>5</sup> Ph. Dubois\*<sup>1</sup>*

<sup>1</sup> Service des Matériaux Polymères et Composites, Université de Mons-Hainaut, Place du Parc 20, B-7000 MONS, Belgium

<sup>2</sup> Laboratoire de Résonance Magnétique Nucléaire, Facultés Universitaires Notre-Dame de la Paix, Rue de Bruxelles 61, B-5000 NAMUR, Belgium

<sup>3</sup> Unité de Microscopie Electronique, Materia Nova Center, Parc Initialis, Avenue N. Copernic 1, B-7000 MONS, Belgium

<sup>4</sup> Laboratoire de Chimie Inorganique Structurale, Université de Liège, Bâtiment B6a, B-4000 LIEGE, Belgium

<sup>5</sup> Centre d'Etude et de Recherche sur les Macromolécules, Université de Liège, Bâtiment B6a, B-4000 LIEGE, Belgium

**Summary:** Morphological and rheological properties of new ternary nanocomposites based on ethylene vinyl acetate copolymers (EVA), commercial organo-modified clays (organoclays) and purified multi-walled carbon nanotubes (MWNTs), prepared via direct melt blending, have been evaluated. For sake of comparison, the corresponding binary compositions, i.e., EVA filled with either organoclays or MWNTs, have been investigated as well. While extensive exfoliation can be observed for binary EVA/clay nanocomposites, the addition of MWNTs appears to limit clay exfoliation. Rheological properties show that both clay and MWNTs increase the elastic modulus of the nanocomposites, reflecting the high degree of nanoparticle interconnectivity that can be found in these materials.

**Keywords:** carbon nanotubes; clay; EVA; nanocomposites; rheology

### Introduction

Homogeneously dispersing rigid particles in polymer matrices is a very common and widely used method that allows for readily increasing the stiffness of the so-obtained composite materials. Depending on the intrinsic nature of the added filler, other properties can also be enhanced such as fire resistance, electrical and thermal properties. However, such improvements of composite materials performances usually require high filling levels [1], detrimental to the ultimate mechanical properties of the resulting materials.

Polymer nanocomposites represent a new class of composite materials, i.e., particle-filled polymers for which at least one dimension of the dispersed particles is in the nanometer range. This variety of fillers provides the related composite materials with significantly improved properties most often at filler content as tiny as 3 to 5 wt%. Interestingly, remarkable thermo-mechanical performances have been recorded using organo-modified layered silicates (organoclays) as nanofiller precursors [2-4]. Actually, upon incorporation of such organoclays in a polymer matrix, intercalation of the polymer chain in-between the clay platelets or complete exfoliation of the silicate platelets can be observed. Exfoliated nanocomposites usually exhibit significantly higher improvement in properties such as mechanical, thermal and flame retardant properties.

First observed by Iijima in 1991 [5], carbon nanotubes is another family of potential nanofillers for polymer matrices. Carbon nanotubes are mainly subdivided in two families: single-walled nanotubes (SWNTs) or multi-walled nanotubes (MWNTs) where several nanotubes of decreasing diameter are interlocked. Carbon nanotubes find applications in various fields such as in field emission devices, electrically and thermally conductive materials, hydrogen storage devices and molecular sieves [6-8]. Even though carbon nanotubes have already been blended within various polymers [9-11], homogeneous dispersion of the nanotubes in the polymer matrix remains one major challenge, since bundles of aggregated SWNTs or MWNTs most often persist and therefore limit the performances of the recovered composite materials. Interestingly, a synergistic effect arising from the combination of carbon nanotubes and organoclays has been recently evidenced [12,13]. Actually, when selected organoclays and MWNTs were blended simultaneously within a soft ethylene vinyl acetate copolymer (EVA) in the molten state, both thermal and flame retardant properties of the so-recovered ternary compositions proved to be much enhanced. In order to shed some light on the origins of such a synergistic effect, it was of prime interest to characterize these nanocomposites and to understand the parameters governing such an original behavior.

In this context, the present work aims at identifying the (nano)morphology of EVA-based compositions filled with selected organoclays and/or purified MWNTs and obtained by direct melt blending. In addition to morphological characterization, the different binary and ternary nanocomposites have been also compared from the point of view of their rheology.

## Experimental Part

### Materials

A commercial ethylene vinyl acetate copolymer (EVA), Escorene UL00328 (Exxon), containing 27wt% of vinyl acetate, was chosen as the matrix. A commercial organoclay, Cloisite®30B, modified by 20.3 wt% of bis(2-hydroxyethyl)methyl tallowalkyl ammonium cation (Southern Clay Products, USA) was used. This montmorillonite has a specific surface area of ca. 750 m<sup>2</sup>/g, with platelets of a thickness around 1 nm. The MWNTs used in this work were produced by catalytic decomposition of acetylene on transition metal particles (Co, Fe) supported on Al<sub>2</sub>O<sub>3</sub>. The catalyst contains 2.5 wt% cobalt and 2.5wt% iron supported on alumina [13]. The synthesis was carried out in a fixed-bed flow reactor at 700°C for reaction time of 60 min. Purified MWNTs were obtained after dissolution of the support in boiling concentrated NaOH water solution and dissolution of the catalysts in concentrated hydrochloric acid water solution. The MWNTs are characterized by an average inner diameter of 5 nm and an average outer diameter of 15 nm, corresponding to ca. 14 - 15 concentric layers. The average length is ca. 50 µm.

### Preparation

EVA/organoclay nanocomposites were compounded on an AGILA two-roll mill for 12 min at 140°C with a friction coefficient equal to 1.35 and a rotation speed of 15 m/s for the slowest roll. EVA/MWNT and EVA/organoclay/MWNT nanocomposites were prepared in a Brabender internal mixer at 140°C, for 12 min with a screw speed of 45 rpm.

### Characterization

XRD was measured using a Siemens D5000 diffractometer with the Cu K $\alpha$  radiation ( $\lambda$  = 0.15406 nm) from 1.5 to 30° by step of 0.04°. Transmission electron micrographs were obtained with a Philips CM200 apparatus using an accelerator voltage of 100 kV. The samples were 70-80 nm-thick and prepared with a LEICA Ultracut UCT ultracryomicrotome cutting at -130°C. Rheological measurements in the melt were obtained in oscillatory mode using disk and plate geometry in a Rheometrics Dynamic Analyser. The measurements were performed at 140°C on disks (diameter = 25 mm and thickness = 3 mm), with a frequency sweep from 15.9 Hz to 0.01 Hz, and 1% strain.

## Results and Discussion

Organo-modified montmorillonites such as Cloisite®30B are known to form nanocomposites with improved fire retardant properties and increased stiffness when dispersed in EVA [14–17]. In a previous study, thermal degradation and tensile properties of binary and ternary blends of EVA with Cloisite®30B and/or MWNTs have been investigated [12]. The properties of the resulting new binary and ternary nanocomposites were enhanced by the presence of both nanofillers. A synergistic effect was observed when the organoclay and MWNTs were added simultaneously: the thermal and flame retardant properties of the related EVA matrices were enhanced.

### Morphological characterization

It was of interest to explore the morphology of these new materials. X-ray diffraction (XRD) and transmission electron microscopy (TEM) were used to identify the nanostructure of these EVA-based composites.

Figure 1 compares the XRD patterns for Cloisite®30B, EVA matrix and EVA-organoclay nanocomposites filled with 1, 3, or 5wt% silicate platelets. The pattern of the pure EVA presents a large peak centered at  $2\theta = 20^\circ$ , characteristic of the crystallinity of the matrix. Although the Cloisite®30B shows a peak centered at  $2\theta = 4.8^\circ$ , characteristic for an interlayer spacing of 18.5 Å, the patterns of the composites based on this organoclay do not show any diffraction peak in the  $1.5 - 10^\circ$  angle region for a filler content below 5wt%. This indicates the disruption/loss of the repetitive structure and thus possibly the exfoliation of the silicate layers. At 5wt% a poorly defined shoulder is observed in the low  $2\theta$  region indicating that some intercalation might remain. Confirming XRD data, the sample containing 3wt% of clay displays a fully exfoliated morphology as observed by TEM (Figure 2). Homogeneously dispersed single clay layers are found in abundance throughout the polymer such that an XRD signal at low  $2\theta$  angle would not be expected.

The XRD patterns for EVA-purified MWNTs composites have also been recorded. Whereas such carbon nanotubes should be characterized by diffraction peaks at  $2\theta = 25.8^\circ$  and  $42.8^\circ$  [11], no diffraction peak was observed in that region (XRD pattern not shown here). TEM micrographs

(Figure 3) show a non homogeneous dispersion of the carbon nanotubes in the EVA matrix. The majority of them are interconnected, exhibiting a high degree of particle-particle entanglements.

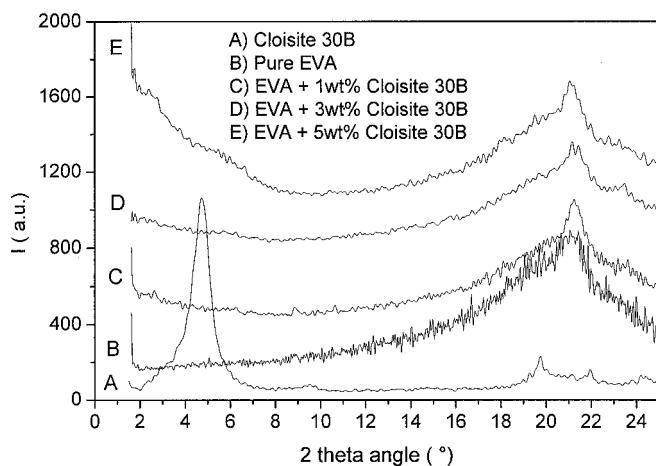


Figure 1. XRD patterns for EVA, Cloisite®30B and binary compositions containing EVA and various amounts of Cloisite®30B.

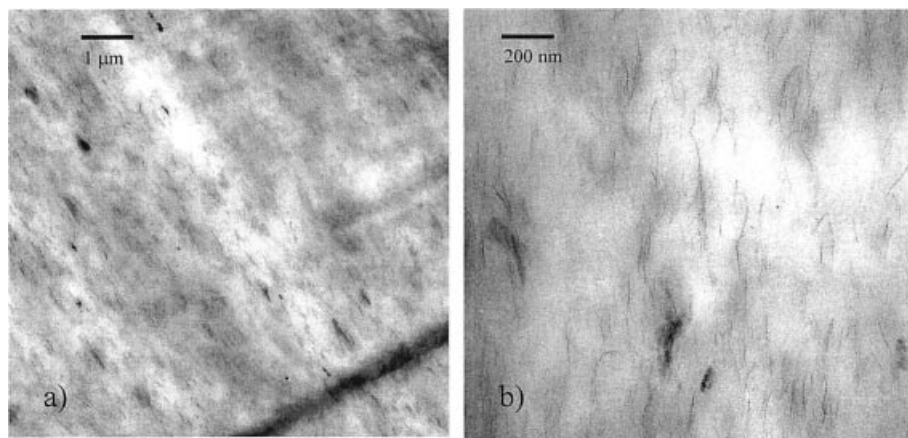


Figure 2. TEM micrographs of a binary system containing EVA and 3wt% Cloisite®30B a) low magnification , b) high magnification.

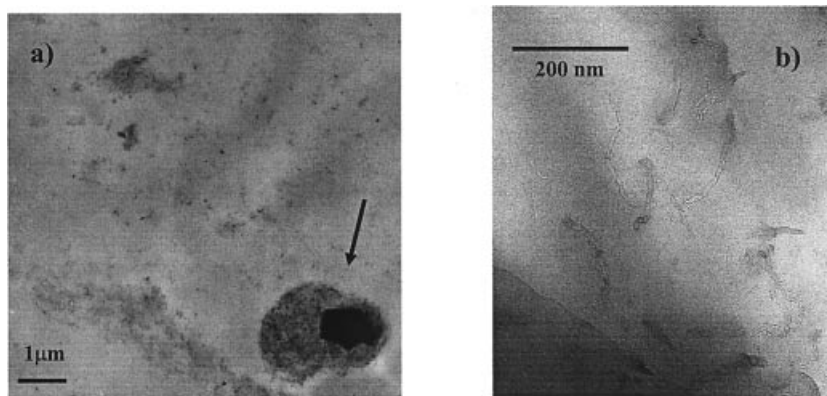


Figure 3. TEM micrographs of a binary system containing EVA and 3wt% MWNTs: a) low magnification with the arrow showing a large aggregate (top view of a MWNTs bundle) b) high magnification showing interconnected MWNTs.

Figure 4 presents the XRD patterns of two ternary nanocomposites both containing 1wt% purified MWNTs and either 2 or 3wt% Cloisite®30B. A diffraction peak in the region of  $2\theta = 6^\circ$  is detected this time for both ternary materials, however more intense in the presence of 3wt% organoclay. A semi-exfoliated semi-intercalated structure is more likely formed despite of the limited quantity of filler (< 5wt%). Carbon nanotubes might be responsible for that observation as they might perturb the good dispersion/delamination of Cloisite®30B in the EVA matrix. Indeed, it is worth reminding that the XRD pattern of the corresponding binary system (again 3wt% Cloisite®30B), thus presented in Figure 1, did not show any diffraction peak at low  $2\theta$  angle. When MWNTs are added with the organoclay, the homogeneity of the platelets dispersion and the extensive exfoliated structure are lost, even at low loading level.

TEM micrographs (Figure 5) of the ternary composite containing 3wt% Cloisite®30B and 1wt% MWNTs confirm XRD observations. Indeed the clay is again exfoliated but not quantitatively. On the other hand, it appears that even though the carbon nanotubes are not fully and homogeneously dispersed in EVA, one can distinguish some individual MWNTs (segments) throughout the sample, again showing rather high degree of interconnectivity. It is worth recalling that the investigated carbon nanotubes are characterized by an average length of 50μm.

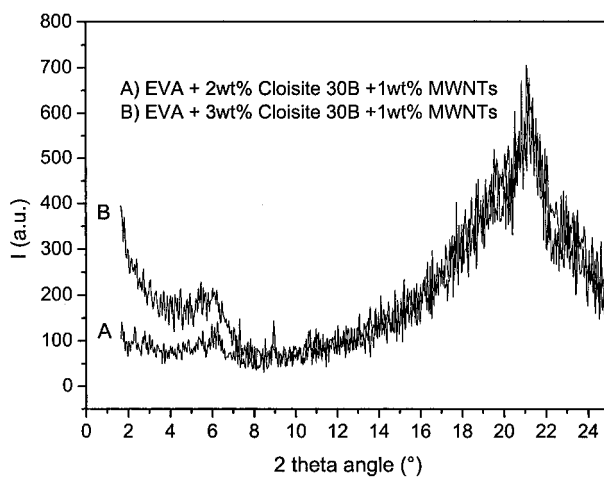


Figure 4. XRD patterns of ternary systems based on 1wt% MWNTs and 2 or 3wt% Cloisite®30B.

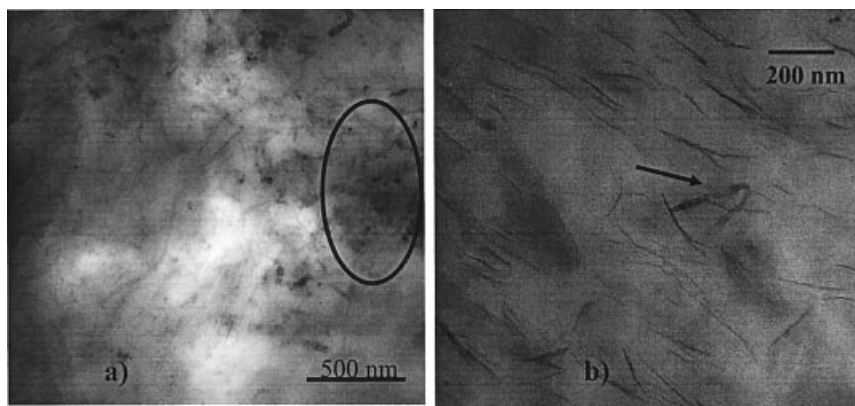


Figure 5. TEM micrographs of a ternary composite (3wt% Cloisite®30B+1wt% MWNTs). a) low magnification showing MWNTs aggregates b) high magnification showing stacks of clay and an isolated carbon nanotubes (a segment of which being highlighted by the arrow).

## Rheological characterization

### Binary systems

Figures 6a and 6b shows the frequency dependence of the storage modulus  $G'$  for various EVA/organo clay and EVA/MWNT binary nanocomposites, respectively. As expected,  $G'$  of the organoclays-based nanocomposites increases with the clay loading on the whole range of swept frequencies (Figure 6a). At high frequencies, the qualitative behavior of  $G'$  is essentially the same whatever the silicate content (all data points turn into parallel lines). However at lower frequencies,  $G'$  increases monotonically with increasing clay content.

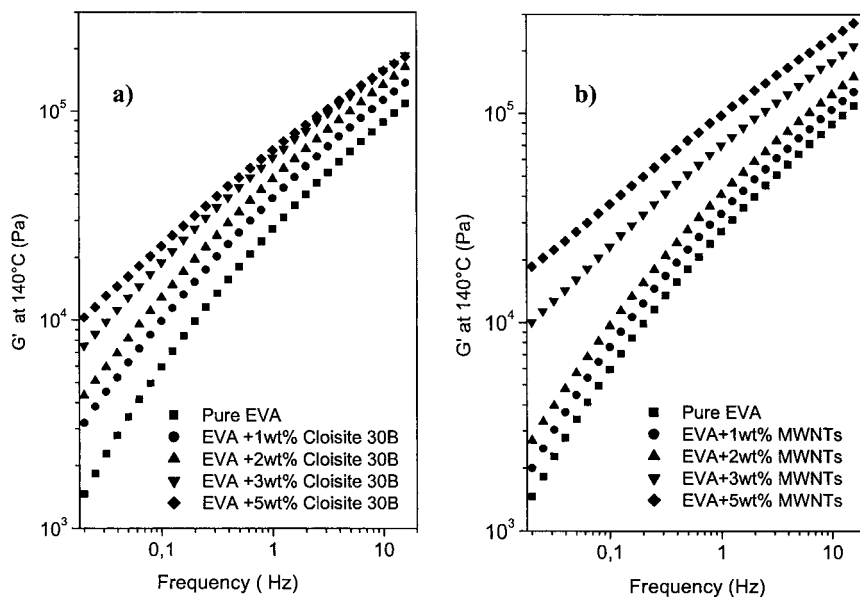


Figure 6. Frequency dependence of the storage modulus  $G'$  for binary nanocomposites at 140°C : a) EVA + Cloisite® 30B, b) EVA + MWNTs.

Above 2wt%, the slope of the storage modulus curve gets less frequency dependent in the whole frequency range. This behavior is characteristic of a non-terminal frequency behavior [18]. This non-terminal behavior, which has also been observed for polystyrene nanocomposites [19] is



attributed to the retardation of molecular relaxation processes produced by the confined geometric effect induced by the presence of highly dispersed nanoclay platelets. Thus a similar observation can be made for the EVA/organoclays nanocomposites. The finely dispersed silicate layers organize in a spatially-linked structure that impedes their free rotation, limiting therefore the relaxation of the material at low deformation frequencies.

For binary nanocomposites based on the purified MWNTs (Figure 6b),  $G'$  increases again with the carbon nanotube content. As the MWNTs content increases in the system and as a consequence of their length (ca.  $50\mu\text{m}$ ), nanotube-nanotube interactions should dominate more and more, eventually leading to percolation and the formation of an interconnected structure of nanotubes. At high concentrations of MWNTs ( $>2\text{wt}\%$ ), connectivity should get more pronounced, as seen in the enhanced elasticity. These particle-particle entanglements give to the material a better resistance against the applied deformation and a substantial increase in  $G'$  is that time observed even at higher frequencies (to be compared to EVA/clay nanocomposites in Figure 6a). The difference observed between the two binary nanocomposites above a filler content of  $2\text{wt}\%$ , is more likely due to the different material morphology and aspect ratio presented by the dispersed silicate platelets and entangled MWNTs.

#### Ternary systems

Figure 7 shows the frequency dependence of  $G'$  evolution recorded at  $140^\circ\text{C}$  for binary and ternary compositions with different loading levels. The rheological behavior of the ternary systems will be discussed in two separate sections:  $G'$  evolution for ternary composites will be compared first with binary systems containing the organoclay and secondly, with binary systems containing the purified MWNTs.

As far as the nanocomposites containing  $3\text{wt}\%$  Cloisite<sup>®</sup>30B are concerned, addition of nanotubes to organoclay leads to a clear modification in the  $G'$  evolution and a significant increase of the storage modulus  $G'$  in the low frequencies region (Figure 7a). This can be explained by the particle-particle entanglements present in the material after the addition of and triggered by the MWNTs. One could therefore assume that the association between such entanglements and the aforementioned spatially-linked structure gives to ternary nanocomposites a better resistance against low deformation. At higher frequencies, the  $G'$  values observed for the ternary composites containing  $2\text{wt}\%$  Cloisite<sup>®</sup>30B and  $1\text{wt}\%$  MWNTs are similar to the binary

material only filled with 2wt% Cloisite®30B. This might result from the limited amount of clay in the ternary composite, likely too low for forming a spatially-linked structure at high frequencies. This is confirmed when looking at the frequency dependent  $G'$  evolution recorded for the ternary nanocomposite containing 3wt% Cloisite®30B and 1wt% MWNTs (Figure 7a). The slope of the curve is relatively constant and the values of  $G'$  are increased in the whole frequency range.

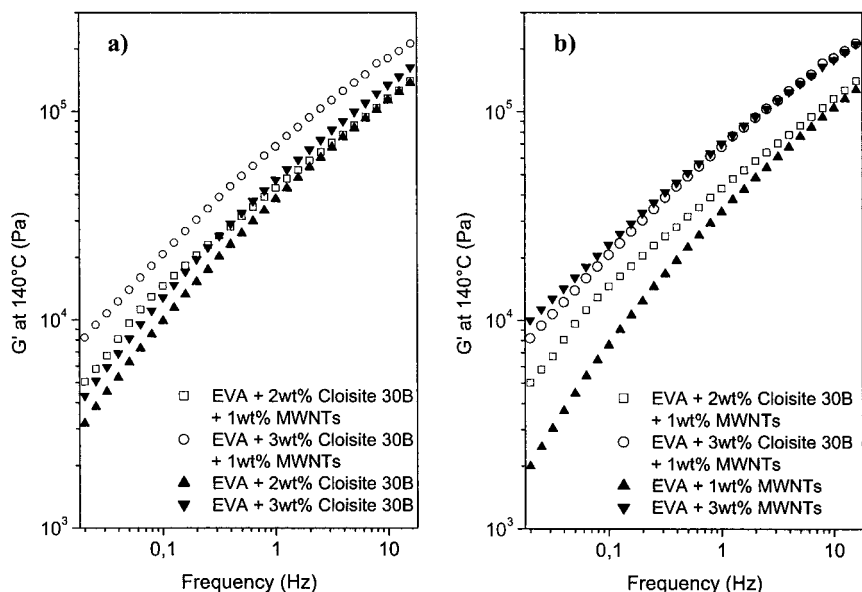


Figure 7. Frequency dependence of  $G'$  evolution at 140°C for binary and ternary systems a) comparison with EVA/organoclay binary compositions; b) comparison with EVA/MWNTs binary compositions.

Secondly, for the nanocomposites containing 3wt% of MWNTs, addition of clay platelets leads to a decrease of  $G'$  values in the whole frequency range as well as some modification in the slope of the evolution curve (Figure 7b). The conclusions are globally the same as above: a sufficient number of nanotube entanglements and a spatially-linked structure built by the homogeneously

dispersed organoclays are required to give a good resistance to the material against high deformations. When the ternary composite contains 3wt% Cloisite® 30B and 1wt% MWNTs,  $G'$  values are equivalent to those recorded for the binary system containing 3wt% MWNTs. In that sample, the spatially-linked structure formed at this clay relative content can thus be reinforced by the addition of a small quantity of carbon nanotubes.

## Conclusions

A new type of materials based on a soft polymer matrix, i.e., ethylene vinyl acetate copolymer (EVA) filled with organoclays and multi-walled carbon nanotubes, actually flake-like (2-D) and rod-like (1-D) nanofillers, respectively, have been prepared via direct melt blending. Our study was focused on the characterization of the material morphology and the rheological behavior in order to better understand the previously observed improvement for properties like the increased thermal stability, mechanical performances and flame retardant behavior [12].

This work confirms that exfoliated nanocomposites based on EVA and organoclay can be prepared by direct melt blending. XRD results, when properly interpreted and combined with TEM results, give a much clearer picture of the nanoscale dispersion and overall global dispersion of the filler in the polymer matrix. While long carbon nanotubes are extremely difficult to disperse in EVA, actually forming well-known associated bundles, the simultaneous addition of clay and carbon nanotubes gives a particular morphology: not totally exfoliated clay platelets and partially dispersed long nanotubes with high degree of interconnectivity. The enhanced elastic melt properties, represented by the increase of the storage modulus  $G'$ , are also particular when the two fillers are simultaneously added. This rheological response is sensitive to the clay amount and related spatially-linked structure, as well as the MWNTs interconnectivity.

## Acknowledgments

The authors wish to thank « Région Wallonne » for financial support in the frame of the Nanotechnology project: BINANOCO. This work was partly supported by the Belgian Federal Government Office of Science Policy (SSTC-PAI 5/3). M.A. and Ph.D. are much indebted to both « Région Wallonne » and European Community “FSE and FEDER” for financial support in the frame of Objectif-1 Hainaut : Materia Nova.

- [1] Rothon R.; *Particulate-Filled Polymer Composites*, 1st ed. Harlow: Longman Scientific; 1995.
- [2] Giannelis EP; *Adv Mater* 1996; 8: 29-35.
- [3] Alexandre M, Dubois Ph; *Mater Sci Eng* 2000; R28: 1-63.
- [4] Pinnavaia TJ, Beall GW; *Polymer-clay nanocomposites*, in "Wiley series in polymer science", Chichester : John Wiley and Sons, 2000.
- [5] Ijima S; *Nature* 1991; 354: 56-58.
- [6] Ajayan PM; *Chem Rev* 1999; 99: 1787-1799.
- [7] Baughman RH, Zakhidov AA, de Heer WA; *Science* 2002; 297: 787-792.
- [8] Thostenson ET, Ren ZF, Chou TW; *Comp Sci Tech* 2001; 61: 1899-1912.
- [9] Andrews R, Jacques D, Minot M, Rantell T; *Macromol Mater Eng* 2002; 287: 395-403.
- [10] Kashiwagi T, Grulke, E, Hilding J, Harris R, Awad W, Douglas J; *Macromol Rapid Commun* 2002; 23: 761-765.
- [11] Pirlot C, Willems I, Fonseca A, BNagy J, Delhalle J; *Adv Eng Mater* 2002; 4: 109-114.
- [12] Peeterbroeck S, Alexandre M, BNagy J, Pirlot C, Fonseca A, Moreau N, Philippin G, Delhalle J, Mekhalif Z, Sporken R, Beyer G, Dubois Ph; *Comp Sci Tech*, 2004, in press
- [13] Beyer G; *Fire Mater* 2002; 26: 291-293.
- [14] Alexandre M, Beyer G, Henrist C, Cloots R, Rulmont A, Jérôme R, Dubois Ph; *Macromol Rapid Commun* 2001; 22: 643-646, and *Chem Mater* 2001; 13: 3830-3832.
- [15] Zanetti M, Camino G, Thomann R, Mülhaupt R; *Polymer* 2001; 42: 4501-4507.
- [16] Tang Y, Hu Y, Wang SF, Gui Z, Chen Z, Fan WC; *Polym Deg Stab* 2002; 78: 555-559.
- [17] Duquesne S, Jama C, Lebras M, Delobel R, Recourt P, Gloagen JM; *Comp Sci Tech* 2003; 63, 1141-1148.
- [18] Riva A, Zanetti M, Braglia M, Camino G, Falqui L; *Polym Degrad Stab* 2002; 77: 299-304.
- [19] Lim YT, Ok Park O; *Macromol Rapid Commun* 2000; 21: 231-235.